Dependence of the quality factor of micromachined silicon beam resonators on pressure and geometry

F. R. Blom,[a] S. Bouwstra, M. Elwenspoek, J. H. J. Fluitman
MESA-Research Institute, University of Twente, P.O. Box 217, 7500 AE Enschede, The Netherlands

(Received 22 May 1990; accepted 5 October 1991)

An experimental study of damping and frequency of vibrating small cantilever beams in their lowest eigenstate is presented. The cantilever beams are fabricated from monocrystalline silicon by means of micromachining methods. Their size is a few millimeters in length, a few 100 μm in width, and a few 10 μm in thickness. Damping and resonance frequency are studied as a function of the ambient pressure p (1–10^5 Pa) and the geometry of the beam. The purpose of this research was to obtain design rules for sensors employing vibrating beams. The analysis of the experimental results in terms of a semiqualitative model reveals that one can distinguish three mechanisms for the pressure dependence of the damping: viscous, molecular, and intrinsic. For viscous damping a turbulent boundary layer dominates the damping at high pressures ($\approx 10^5$ Pa), while at smaller pressure laminar flow dominates. In the latter region, this leads to a plateau for the quality factor Q and in the former to $Q \alpha \sqrt{p}$. The pressure p_c at which the transition from laminar flow dominated damping to turbulent flow dominated damping occurs depends on the geometry of the beams. p_c is independent on the length and decreases with both, the width and the thickness of the beams.

I. INTRODUCTION

Micromachined silicon structures, such as beams and diaphragms, currently find their way in sensor research. The reasons are obvious: silicon is mechanically a strong material and the structures can be made using anisotropic etching techniques.[1] Moreover, the processes of the integrated circuit (IC) fabrication can be used to build small scale sensors out of these structures, and the same silicon can be used to integrate the required electronics as well.

In our research we are interested in resonant silicon microstructures, used in frequency-output sensors.[2] This is a growing area of interest, thanks to the advantages of this class of sensors.[3] The resolution of a frequency-output sensor is mainly determined by the mechanical quality factor; the higher the quality factor, the sharper the resonance peak, and thus the higher the resolution of the frequency-output sensor.

In determining the mechanical quality factor, several damping mechanisms must be taken into account. Newell[4] concludes in his work on miniaturization of vibrating structures, that damping by air is the most profound one. He distinguishes different damping mechanisms as the air pressure varies, corresponding to the properties of gases at low pressures. Therefore, our research will be concentrated on the pressure dependence of the quality factor. At the same time we shall examine how this dependence varies with the geometry of the resonant beam. The goal aimed at in this article is to find design rules for the geometry of resonant silicon beams in order to obtain a quality factor that is as large as possible at atmospheric conditions. Emission of sound is negligible for the structures under consideration here.[5,6]

Most of the research on the pressure dependence of the damping of vibrating structures in performed on quartz resonators.[7–9] Also theoretical treatments of oscillating vacuum friction gauges used as pressure sensors are found in literature.[10,11] More recently, research on silicon structures used for accelerometers has been reported.[12,13] Mass-beam systems are made in and from silicon, and their quality factor and resonance frequency is measured as a function of air pressure. Although the mechanical description of these systems is the same as that for our structures, the results of the pressure dependence differ strongly due to the large mass of these systems compared to the mass of our beams. The work most related to that described in this article has been done by Kokubun *et al.*, who compare their measurements on quartz tuning forks with a simple damping theory.[8,9,14,15] Although they find good agreement, they do not find a quantitative relation between the quality factor and the tuning fork geometry.

In this study we concentrate ourselves on beams vibrating perpendicular to the substrate. Surfaces except the one-end support are very far away and will not influence the damping. This is very much different from resonators described by Howe *et al.*, which are very close to the substrate (a few micron) and vibrate either perpendicular[16] to the substrate or in plane with the substrate.[17] Obviously the viscous damping is very much different in those designs. Applications of perpendicular vibrating silicon beams are, e.g., a resonating force sensor[18] or a resonating microbridge mass flow sensor.[19]

In the theoretical section of this article, expressions are derived for the damped resonance frequency and the quality factor of a slightly damped vibrating beam, and for the pressure dependence of both parameters. The considered pres-

sure range (10^{-2}–10^{5} Pa) is divided into three regions, an intrinsic, a molecular, and a viscous region, according to Newell[4] and Drawin.[11] Each region has its own dominant damping mechanism. In order to derive analytical expressions in the viscous region, the beam will be approximated by a sphere. As will be seen later, this rather crude approximation serves for a good qualitative and an even reasonable quantitative understanding of the experimental results. In the next sections, the experiments, their results, and a discussion will be given.

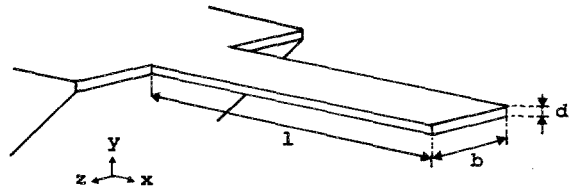

FIG. 1. Drawing of the micromachined silicon cantilever beam.

II. THEORY

A. The quality factor and resonance frequencies of a damped resonant beam

1. Definition of the quality factor

The following definition for the quality factor of a damped system is used[20]

$$Q=\frac{2\pi(\text{stored vibration energy})}{\text{dissipated energy per period}}=\frac{2\pi U_i}{U_d}. \tag{1}$$

In case of weak damping it can be shown that Q can be measured by determining the logarithmic decrement of the vibration, from the amplitude of vibration at resonance with respect to the static amplitude, or from the bandwidth at resonance. The last one will be used in our case to measure the quality factor of our resonant beams.

2. Drag force

The drag force P is the force exerted on the vibrating beam by the surrounding medium (i.e., air). Writing the velocity of the vibrating beam in the complex form $u=u_0e^{j\omega t}$, we obtain a complex drag force proportional to the velocity[5] $p=(\beta_1+j\beta_2)u$, with β_1 and β_2 (real) constants. For harmonic motion this expression can be written as the sum of two terms with real coefficients

$$P=(\beta_1+j\beta_2)u=\beta_1u-\beta_2u/\omega. \tag{2}$$

The part of the drag proportional to the velocity u is called the dissipative part, because it leads to energy dissipation; the other part, proportional to the acceleration $\dot{u}$, is called the inertial part.

3. The resonance frequency of a damped vibrating beam

Consider a cantilever beam of length l, width b, and thickness d vibrating in a flexural motion in a fluid medium, which exercises the previously described drag force upon the beam (see Fig. 1). If we neglect the influence of shear deformation and if no distributed loads are present, the free motion of this prismatic, homogeneous beam is described by (using standard mechanics[21])

$$\frac{EI}{l^4}\frac{\partial^4y(\eta,t)}{\partial\eta^4}+f_1\frac{\partial y(\eta,t)}{\partial t}+(\rho_sA+f_2)\frac{\partial^2y(\eta,t)}{\partial t^2}=0, \tag{3}$$

where $\eta=x/l$: the normalized length parameter; E: the Young modulus; I: the moment of inertia (i.e., $bd^3/12$); f_1: the dissipative drag parameter per unit length ($f_1=\beta_1/1$); f_2: the inertial drag parameter per unit length ($f_2=\beta_2/\omega l$); ρ_s: the density of the beam material (i.e., silicon); A: the cross-sectional area of the beam (i.e., bd).

Since the drag force is only defined cf. Eq. (2) for harmonic motion, Eq. (3) is only valid for harmonic solutions of the vibration. It is seen from Eq. (3) that the inertial part of the drag force has apparently the effect of increasing the mass of the vibrating beam. Solving Eq. (3) under the condition of resonance yields the eigenvalues for the damped angular resonance frequencies ω_{dn}

$$\omega_{dn}=\left[\frac{EIk_n^4}{(\rho_sA+f_2)l^4}-\frac{1}{4}\left(\frac{f_1}{\rho_sA+f_2}\right)^2\right]^{1/2}, \tag{4}$$

where k_n is the constant for the nth order mode of resonance.

The damping parameter f_1 is small for vibrations in gases, thus the second term under the square root may be neglected. Moreover, since ρ_sA is much larger than f_2, the damped resonance frequency of a vibrating beam is approximated by

$$\omega_{dn}\simeq\left(\frac{EIk_n^4}{(\rho_sA+f_2)l_4}\right)^{1/2}\simeq\omega_n\left(1-\frac{1}{2}\frac{f_2}{\rho_sA}\right), \tag{5}$$

where ω_n is the nth order undamped angular resonance frequency, given by:

$$\omega_n=2\pi f_n=k_n^2\frac{d}{l^2}\sqrt{\frac{E}{12\rho_s}}. \tag{6}$$

For the first-order resonance $k_0=1.875$ for a cantilever beam.[21]

4. The mechanical quality factor of a damped vibrating beam

Using Eq. (1) the quality factor Q of a slightly damped vibrating beam can be determined. The stored vibration energy is equal to the maximum value of the kinetic energy. Using separation of the variables η and t and considering only harmonic motion, thus

$$y(\eta,t)=w(\eta)Y(t)=w(\eta)e^{j\omega t}, \tag{7}$$

we obtain for U_i

$$U_i=(U_{\text{kin}})_{\max}=\int_0^1\frac{1}{2}l(\rho_sA+f_2)\left|\left(\frac{\partial y(\eta,t)}{\partial t}\right)^2\right|_{\max}d\eta$$

$$=\frac{1}{2}l(\rho_sA+f_2)\omega^2\int_0^1w^2(\eta)\,d\eta. \tag{8}$$

The dissipated energy per period U_d or the damping energy, is given by the product of the dissipative part of the drag force P and the velocity u

$$U_d = \int_0^T Pu\,dt = \int_0^1 \int_0^T lf_1 \left(\frac{\partial y(\eta,t)}{\partial t} \right)^2 dt\,d\eta \tag{9}$$

with $T = 2\pi/\omega$, the period time.

Substituting Eqs. (8) and (9) into Eq. (1) and using Eq. (7), we get for the quality factor Q

$$Q = \frac{2\pi \tfrac{1}{2} l(\rho_s A + f_2)\omega^2 \int_0^1 w^2(\eta)\,d\eta}{lf_1\omega^2 \int_0^1 w^2(\eta) \int_0^T \cos^2 \omega t\,dt\,d\eta}, \tag{10}$$

The time integral gives π/ω and so Q can be calculated without knowing the exact mode shape function $w(\eta)$ to arrive at, with $f_2 \ll \rho_s A$

$$Q = \rho_s A\omega/f_1. \tag{11}$$

Here ω is the damped angular resonance frequency ω_{dn} of Eq. (5).

B. Pressure dependence

1. Superposition of damping mechanisms

The parameters which are pressure dependent in the basic equation of our resonant system, Eq. (3), are the damping parameters f_1 and f_2. In order to analyze how Q and ω_{dn} vary with air pressure, the pressure range from vacuum to atmospheric pressure can be divided into several regions. These can be named after the dominant damping mechanism in each region:[4,11] the intrinsic, the molecular, and the viscous region.

If all the damping mechanisms acting on the vibrating system are proportional to the velocity of the vibration, the total drag force consists of contributions of the separate mechanisms. Accordingly, the damping parameters β_1 and β_2 can be written as the sum of the several parameters.

$$\begin{aligned} P &= P_a + P_b + \cdots \\ &= (\beta_{a1} + j\beta_{a2})u + (\beta_{b1} + j\beta_{b2})u + \cdots \\ &= (\beta_1 + j\beta_2)u. \end{aligned} \tag{12}$$

In the derivation of the quality factor of such a composed system, we are only interested in the dissipative part of the drag force. Combining Eqs. (1), (9), and (12), the quality factor can be written as:

$$\frac{1}{Q} = \frac{1}{Q_1} + \frac{1}{Q_2} + \cdots = \sum_i \frac{1}{Q_i}. \tag{13}$$

From this equation it is obvious that the value of Q cannot exceed the value of the smallest specific Q_i. Instead of actually calculating the total damping parameters in every region, they may be approximated by the damping parameters that are dominant in that region.

2. The intrinsic region

In the intrinsic region air pressure is so low that air damping is negligible compared to the intrinsic damping of the vibrating beam itself. Then both f_1 and the corresponding Q are independent of air pressure and beam geometry, and Q reaches a maximum value. Furthermore, f_2 equals zero and thus $\omega_{dn} = \omega_n$.

3. The molecular region

In the second region, the molecular or Knudsen region, the damping is caused by independent collisions of noninteracting air molecules with the moving surface of the vibrating beam. In this case the drag force can be determined by means of the kinetic theory of gases. It follows that the damping parameter f_1 is proportional to the air pressure p and the width of the beam b [11]

$$f_1 = k_m bp \tag{14}$$

with

$$k_m = (32M/9\pi RT)^{1/2}, \tag{15}$$

where M, R, and T are the mass of the gas molecules, the gas constant and the absolute temperature, respectively. For air molecules M equals 28.964 gr/mol, so at room temperature ($= 300$ K) $k_m = 3.6 \times 10^{-3}$ s/m.

In this region also $f_2 = 0$ and thus, using Eq. (6) for ω_{dn}, we derive for Q

$$Q = \frac{k_n^2}{k_m p} \left(\frac{d}{l} \right)^2 \left(\frac{\rho_s E}{12} \right)^{1/2}. \tag{16}$$

4. The viscous region

The third or viscous region leads up to atmospheric pressure or further. In this region the air acts as a viscous fluid and the drag force must be calculated using fluid mechanics. Since the velocity of the vibrating beam is always much smaller than the speed of sound in the medium, we may consider the medium as being incompressible.

For the velocity field $\mathbf{u}(x,y,z,t)$ of an incompressible viscous medium the Navier–Stokes equation and the continuity equation are applicable[5]

$$\frac{\partial \mathbf{u}}{\partial t} + (\mathbf{u} \cdot \operatorname{grad})\mathbf{u} = -\frac{1}{\rho_0} \operatorname{grad} p + \frac{\mu}{\rho_0} \Delta \mathbf{u}, \tag{17}$$

$$\operatorname{div} \mathbf{u} = 0, \tag{18}$$

with μ and ρ_0 the dynamic viscosity and the density of the medium, respectively. In the pressure region under consideration we may assume μ to be a constant (N.B. we assume ideal gases, so $\rho_0 = M/RT \cdot p$).

It is rather difficult to determine the exact velocity field around the vibrating beam. Only for simple bodies an analytical expression for $\mathbf{u}$ can be derived from these two equations. However, Kokubun *et al.*[8,15] have proposed an approximation for the damping problem of a vibrating quartz tuning fork. They considered the tines of the fork with an almost quadratic cross section as a string of spheres. If these spheres vibrate independently of each other, with infinite separation, the resulting drag force is the sum of the drag forces of the single spheres. Their measurements agreed well with the theoretical predictions. For our case it could be

more appropriate to model the beams by discs rather than spheres, however, according to Lamb,[22] the drag force on a disc moving perpendicular to its surface is very close to that of a moving sphere. We shall comment on this matter below and use the sphere model.

In case of small Reynolds numbers, the drag force for an oscillatory motion of a sphere with radius R can be calculated straightforwardly from the Navier–Stokes Eq. (17) and the continuity Eq. (18). Thus, the parameters β_1 and β_2 of Eq. (2) are determined[5]

$$\beta_1 = 6\pi\mu R(1 + R/\delta), \tag{19}$$

$$\beta_2/\omega = (2/3)\pi R^3 \rho_0\left(1 + \frac{9}{2}\frac{\delta}{R}\right). \tag{20}$$

Here δ is the width of a boundary layer perpendicular to the direction of the motion and is a measure for the depth of penetration of a lateral wave. In this region there is a nonvanishing curl of the velocity field which means that this region is turbulent; the air flow is rotational instead of potential. The width δ is dependent on the pressure and given by

$$\delta = (2\mu/\rho_0\omega)^{1/2}. \tag{21}$$

The first expression on the right-hand side of Eq. (19) equals Stokes' equation for static flow passing a sphere (or for a sphere in uniform motion through a viscous fluid); the second expression is the result of the harmonic motion of the sphere and is dependent on both the resonance frequency of the sphere, as well as the density of the medium [cf. Eq. (21)].

Assuming $\omega_{dn} \simeq \omega_n$, i.e., ignoring the contribution of the additive mass to the quality factor, we can combine Eqs. (6), (11), and (19), and finally obtain for the quality factor of a vibrating beam in the viscous region, approximated by an oscillating sphere with radius R

$$Q = \frac{k_n^2 bd^2(\rho_s E/12)^{1/2}}{6\pi\mu Rl(1 + R/\delta)}. \tag{22}$$

For the relative frequency shift of the first-order resonance frequency we derive, combining Eqs. (5), (6), and (20)

$$\Delta\omega/\omega_0 = -\frac{\pi R^3\rho_0}{3\rho_s lbd}\left(1 + \frac{9}{2}\frac{\delta}{R}\right). \tag{23}$$

Equation (23) [or more often Eq. (5)] is used in literature to describe the frequency dependence of resonant pressure sensors.[7] It can be seen from Eqs. (22) and (23) that for both Q and $\Delta\omega/\omega_0$ two regions are recognized, depending on the ratio R/δ

for $R/\delta \ll 1$: Q is independent of p,
for $R/\delta \gg 1$: Q is proportional to $1/\sqrt{p}$,
for $R/\delta \gg 9/2$ $\Delta\omega/\omega_0$ proportional to p,
for $R/\delta \ll 9/2$ $\Delta\omega/\omega_0$ proportional to $\sqrt{p}$.

At this stage we define the critical pressure p_c as the pressure at which R equals δ. As stated in the Introduction, we will put emphasis on making Q as large as possible at atmospheric conditions. This means that the dependence of this p_c on the beam dimensions must be determined in order to shift p_c as far as possible above 10^5 Pa. In that case Q will have the maximum value for the viscous region, which is independent of pressure.

Kokubun *et al.*[15] refined the model by introducing Millikan's slip theory[23,24] (see also Ref. 10) which accounts for the fact that at low pressure the velocity of the moving surface does not equal the velocity of the fluid at the surface. This effect is important if the linear dimensions of the moving object becomes comparable to the mean free path of the molecules in the fluid. The effect describes the pressure dependence of Q at the transition from the molecular region to the viscous region. Here we ignore this effect because the experimental uncertainty is too large to make the slip effect visible.

TABLE I. Dimensions of the beams used (length l, width b, and thickness d), their first-order resonance frequency f_0 and calculated results of the curve fitting for the radius R of a sphere and the critical pressure p_c.

Sample	l (mm)	b (mm)	d (μm) (± 1)	f_0 (Hz) (± 1)	R (μm) (± 40)	p_c (Pa) (± 40)
7-3	1.5	0.5	9	5259	165	35
7-4	3.0	0.5	10	1491	310	55
7-5	2.0	0.5	10	3163	255	25
85-1	4.0	0.5	15	1310	370	30
85-3	4.0	0.5	15	1242	390	25
85-4	4.0	0.4	14	1193	355	35
85-6	4.0	0.4	14	1223	360	30
85-9	4.0	0.3	12	1005	230	100
85-10	4.0	0.2	11	915	160	210
85-12	4.0	0.2	12	1017	155	200
89 B2	1.4	0.2	5	3751	80	195
89 B5	1.4	0.4	6	3995	120	90
89 B6	1.4	0.4	6	3978	140	65
89 B8	1.4	0.6	6	3832	160	50
90 F5	2.0	0.4	13	4537	175	35
91 C5	2.8	0.4	34	5952	300	10

III. EXPERIMENTS

A. Samples and experimental setup

Several batches of silicon cantilever beams were made using anisotropic etching of silicon in a KOH solution and photolithographic techniques. The beams of the different batches have varying geometries. The beams used are listed in Table I, together with their dimensions and resonance frequencies. Figure 2 shows a microphotograph of a realized silicon cantilever beam (sample 7-4).

The experimental setup consists of a sample holder with a mechanical exciter, placed in a vacuum chamber, a Michelson interferometer, a Photodyne, and a HP4194A impedance/gain-phase analyzer, as is schematically drawn in Fig. 3. The whole setup is placed on a heavily damped table.

Together with its frame, the exciter, a loudspeaker, is mounted on a microcontrolled xyz table in order to position the appropriate beam in the spot of the laser beam. The xyz

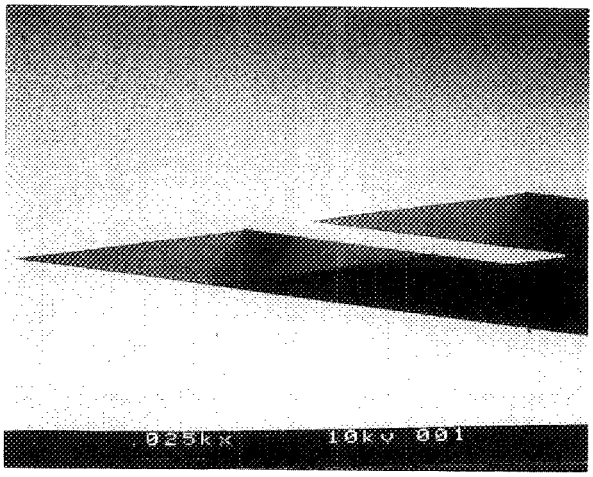

FIG. 2. Microphotograph of a realized silicon cantilever beam with length = 3.0 mm, width = 0.5 mm, and thickness = 7 μm (sample 7-4).

table is firmly attached to the mechanical table. The sample is mounted on the membrane of the loudspeaker by means of mechanical clamps. Using the gain-phase analyzer an ac voltage is applied to the loudspeaker, which will result in vibrations of the beams due to inertial forces. The vibration is contactlessly detected by the interferometer, resulting in a modulation of the light intensity. The photodyne transforms this optical signal into an electrical signal, which is fed into the input of the gain-phase analyzer.

The vacuum chamber can be pumped down to a pressure of about 10^{-3} Pa by means of an oil diffusion pump backed by a rotary pump. The pressure inside the chamber is measured with a Pirani gauge and a Bourdon tube. Air is used as fluid medium. The cylindrical chamber has a radius of 15 cm and a height of 40 cm.

B. Measurement method

The resonance frequency is found by sweeping the excitation frequency with the gain-phase analyzer. The vibration amplitude of the samples is kept small, usually below 80 nm, in order to avoid nonlinear damping mechanisms (i.e., turbulency). Furthermore, in this case the Michelson interferometer operates in an almost linear regime.

In order to determine the frequency characteristic of the whole setup, the transfer function was measured using a rigid silicon wafer as sample. These measurements revealed the resonances of the measurement setup. Although some peaks appeared in the kilohertz region, most of the distortion is located below 1 kHz. In the case of ambiguity in determining which peak belongs to the beam to be measured and which one to the setup, a reference measurement can be performed. This difference measurement can also be performed automatically. It turned out that within the range of the resonance frequencies of the beams the transfer of the setup can be considered frequency independent within the small bandwidth used (i.e., 20 Hz).

The quality factor is found from the transfer plots of the gain-phase analyzer by measuring the bandwidth between the two -3 dB points in this characteristic. Most points were determined from the phase transfer (i.e., + and $-45°$ phase shift), rather than the amplitude transfer, because these appeared to be less sensitive to distortions. Q is calculated from this bandwidth and the resonance frequency.

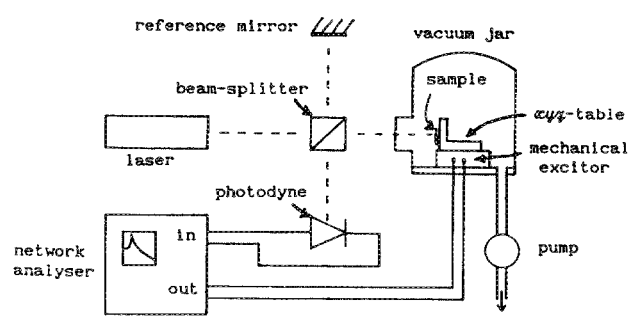

FIG. 3. Sketch of the experimental setup.

IV. RESULTS AND DISCUSSION

A. Measurements of the resonance frequency

From the Eqs. (5) and (6) it can be seen that the damped resonance frequency is proportional to d/l^2. In Fig. 4 the results are shown for f_{d0}, the first-order damped resonance frequency, versus d/l^2, measured at atmospheric pressure. Also the theoretical line is shown and we see a good agreement between measurements and theory. The (sometimes) large error results from the uncertainty in the thickness of the beams of ± 1 μm. As will be seen later, the difference between the damped and undamped resonance frequency is much smaller than this error.

In Fig. 5 the results for $\Delta\omega/\omega_0$ versus p are depicted, together with the theoretical linear relation according to Eq. (5). The slope of the curves of $\Delta\omega/\omega_0$ versus p somewhat smaller than 1. Furthermore, for our geometries $\Delta\omega/\omega_0$ has a maximum value of approximately 1% at 10^5 Pa. This means that indeed $f_2 \ll \rho_s A$.

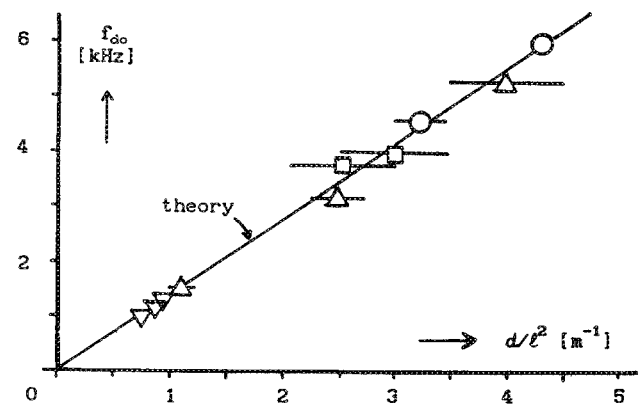

FIG. 4. Results of the damped resonance frequency f_{d0} as function of the dimensional parameter d/l^2 for the cantilever beams. The drawn line is according to theory, cf. Eq. (6).

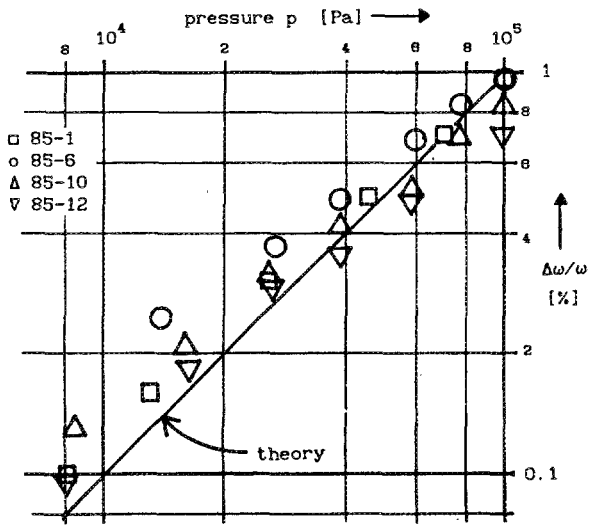

FIG. 5. Relative frequency shift $\Delta\omega/\omega_0$ as a function of the pressure. The drawn line is according to theory, cf. Eq. (5).

B. Pressure dependence of the quality factor

In order to make it possible to compare the results of beams with different lengths and thicknesses the value of the measured Q is normalized with the aid of Eqs. (6) and (11), setting $R = b$. So in Fig. 6, $Q(l/d)^2$ is shown as a function of air pressure p in the pressure range from 10^{-2} to 10^5 Pa for beams having the same width. In this graph the theoretical lines for the molecular and viscous region are drawn as well, according to Eq. (16) and the pressure independent part of Eq. (22), respectively.

Below $p = 1$ Pa there is the intrinsic region. For beam 7.3 for instance, we find an intrinsic Q of approximately 2×10^5, which is comparable with the quality factor of quartz resonators in high vacuum. Between $p = 1$ and $p = 100$ Pa we find the molecular region, where Q is proportional to $1/p$, cf. Eq. (16). Above $p = 100$ Pa there is the viscous region: first Q is independent of pressure, but at atmospheric pressure Q is almost proportional to $\sqrt{p}$, cf. Eq. (22). Here the graphs deviate from each other due to the different geometries, which result in different resonance frequencies, and thus, in different values for the boundary layer thickness δ.

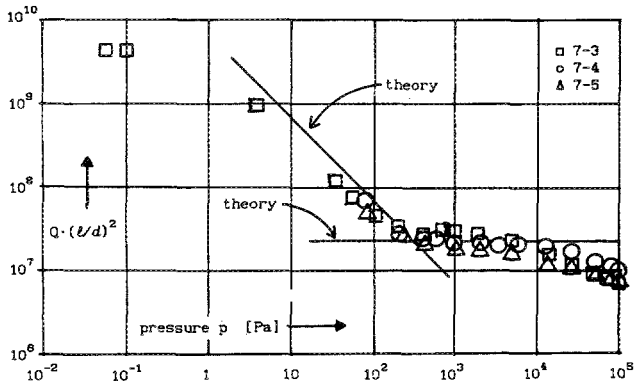

FIG. 6. Normalized quality factor $Q[= Q(l/d)^2]$ vs the pressure p in the pressure range from 10^{-2}–10^{-5} Pa for several beams with different lengths. The theoretical prediction of the dependence of Q on p when the damping by air dominates is drawn [Eq. (16) and pressure independent part of Eq. (22), setting $R = b$].

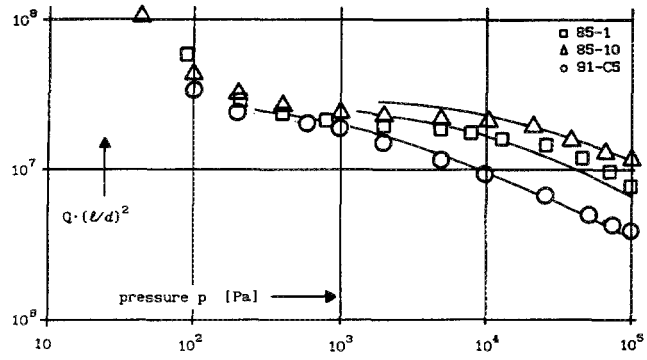

FIG. 7. Normalized Q vs p in the viscous region for beams with different dimensions. Drawn lines are fits.

In Fig. 7 other results of $Q(l/d)^2$ versus p are shown for the pressure range between 10 and 10^5 Pa, i.e., the viscous region. In this graph other dimensions are varied than those in Fig. 6. In comparison with the results of other researchers in this field,[7-9] we observe a relatively wide region, where Q is independent of p. This phenomenon is related to the dimensions of the beams. The upper limit of this region is governed by the critical pressure p_c, i.e., the pressure where $R = \delta$. This pressure is dependent on the resonance frequency of the beam, as can be seen from Eq. (21). In the next subsection we shall discuss the dependence of p_c on the dimensions of the beam more thoroughly.

C. Determination of the critical pressure

1. Curve fitting

As stated in the Introduction of this article our goal is to obtain an as large as possible value for the quality factor at atmospheric conditions. As explained in the former subsections this Q is dependent on the critical pressure p_c. If we can make $p_c > 10^5$ Pa, only Stokes' damping will remain and Q will have a maximum value, which is independent of pressure.

In order to investigate the dependence of p_c on the dimensions of the beam, the measurements of several batches are combined and curve fitting is performed. In this case Eq. (22) is used, following the description of Kokubun.[8] For the curve fitting a least squares method is used.

2. Results

The results of these calculations for the beams of the different batches are listed in Table I. Here, apart from the dimensions and damped resonance frequencies of the beams used, the best fit value for the radius of the sphere R and the corresponding critical pressure p_c are given. In Fig. 8, these data are plotted as a function of the dimensions of the beams.

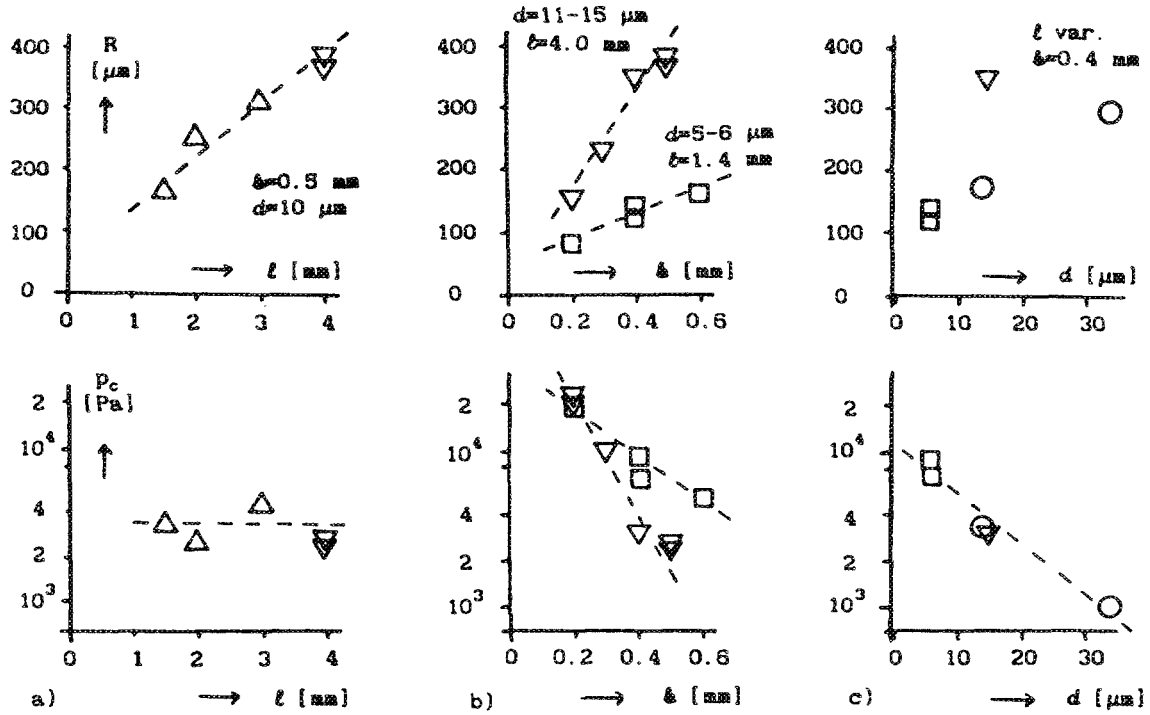

FIG. 8. Results of the curve fitting from measurements of the quality factor. Shown is the best fit radius R of a sphere and the critical pressure p_c vs (a) the length l of the beam; (b) the width b of the beam; (c) the thickness d of the beam (extrapolated).

Generally the fit was better for ratios of l/b close to unity. This is quite understandable, since in this case a sphere fits physically better as well.

3. Discussion

It can be concluded from Fig. 8 that the length of the beam l has no influence on p_c, whereas p_c decreases strongly with the width of the beam b. The results of Fig. 8(c) are extrapolated from these conclusions. Here results are shown for beams with varying lengths, but the same width. We see that p_c also strongly decreases with increasing thickness d of the beam. As for the dependence of the fit on R, no direct conclusions can be drawn; R tends to increase with each parameter.

In order to get more insight into this dependence, we take a closer look at the physical origin of the parameter R in the drag force parameter β_1 of Eq. (19). As previously stated, the first expression describes the static damping and the first R can therefore be related to the surface area perpendicular to the direction of the motion. Lamb shows in his work on hydrodynamics that the damping of a disc with radius R, moving perpendicularly to this surface equals the damping of a sphere having a radius of $0.85R$.[22] The second expression in Eq. (19) is related to a laterally moving wave. Hence, the second R has some relation with the surface area of the sides of the beam. From this we conclude that a fit function with two individual fit parameters could be more appropriate. However, performing such a fit did not seem to give reasonable new insight, due to the proximity of the transition between the molecular and viscous region.

Hirata *et al.*[9] also investigate the size effect of quartz tuning-fork oscillators on their electrical impedance and found the inverse dependence of the impedance on the width of the tines. However, they only examine the dependence on dimensions at two different pressures, one in the molecular region and the other at 10^5 Pa, which makes it difficult to correlate their results with our own. Moreover, their tines have an almost square cross section, whereas our beams have b/d ratios of ten and more.

From the foregoing discussion we arrive at the design rules for beams with an optimum quality factor at atmospheric pressure. The thickness and the width should be chosen as small as possible in order to obtain a large critical pressure p_c. In that case Q reaches a maximum pressure-independent value in the viscous region. The length of the beam seems to have no effect on p_c. On the other hand, since Q is proportional to the square of d/l, a thick and short beam seems to be more appropriate to obtain a large Q.

V. CONCLUSIONS

In this article we have given a theoretical description for the damped vibrations of cantilever beams. Assuming that the damping is relatively small, the damped resonance frequency was calculated. These calculations were verified by measurements, which also revealed that the relative frequency shift between damped and undamped resonance frequency was 1% at the most. This shift is affected by an apparent increase of the mass of the vibrating beam and it is (almost) proportional to the pressure p.

In our theory we assume the damping by the medium to be the dominant mechanism, and hence it is based on fluid dynamics and the kinematic theory of gases. This is confirmed

by measurements, which showed that the pressure range can be divided into four regions, each with its own dominant damping mechanism.

Below 1 Pa the damping is intrinsic of origin and so Q is independent of p. For our beams very high Q values in the order of 2×10^5 were measured in this region. Between 1 and 100 Pa, the molecular region, the damping is determined by the independent collisions of molecules with the vibrating beam surface. In this region, Q is proportional to $1/p$.

The third and fourth region are both viscous from origin, but the former is governed by the static Stokes' damping, whereas in the latter the harmonic damping in a boundary layer is dominant. In these regions, Q is independent of p and proportional to $\sqrt{p}$, respectively. The transition between the last two mentioned regions is at the critical pressure p_c.

All the beams considered so far had a mechanical quality factor larger than 100 at atmospheric pressure. Assuming a resonance frequency of several kilohertz, the frequency resolution is in the order of several tens of hertz. This is rather large when a high resolution frequency-output sensor is required. A quality factor in the order of several thousands would be more desirable in this case.

By approximating the cantilever beam by a sphere, an analytical expression for Q is derived, which was used in a curve-fitting program. In this manner the dependence of p_c on the beam dimensions was investigated. Generally, the fit was better for ratios of l/b close to unity. The fit relation used actually contains two fit parameters, the first related to the surface area perpendicular to the direction of vibration and the second to the surface area of the sides of the beam. Therefore, a fit function with two individual fit parameters would be more appropriate.

Finally, the design rules for a large mechanical quality factor at atmospheric pressure are obtained; a wider and thinner beam increases the critical pressure p_c and a thicker and shorter beam increases Q.

ACKNOWLEDGMENTS

We want to thank R. M. de Vink, A. Versluijs, A. Prak, and J. D. Baxter for their contribution to this work. This research in the program of the Dutch Foundation for Fundamental Research on Matter (FOM) was sponsored by the Dutch Technology Foundation (STW).

[a] Currently working at Océ Nederland b.v., R&D Department, P.O. Box 101, 5900 MA Venlo, The Netherlands.

[1] K. Petersen, IEEE Proc. **70**, 420 (1982).
[2] See for example J. G. Smits *et al.*, Sensors Actuators **4**, 565 (1983); F. R. Blom *et al.*, *ibid.* **17**, 513 (1989).
[3] R. T. Howe, Proceedings of the 4th International Conference on Solid State Sensors and Actuators (Transducers'87) Tokyo, Japan, 1987 (unpublished), pp. 843–848.
[4] W. E. Newell, Science **161**, 1320 (1968).
[5] L. D. Landau and E. M. Lifshitz, *Fluid Mechanics*, Course of Theoretical Physics Vol. 6, 2nd ed. (Pergamon, Oxford, 1963), pp. 88–96.
[6] R. K. Jeyapalan and E. J. Richards, J. Sound Vib. **67**, 55 (1979).
[7] M. Christen, Sensors Actuators **4**, 555 (1983).
[8] K. Kokubun, M. Hirata, H. Murakami, Y. Toda, and M. Ono, Vacuum **34**, 731 (1984).
[9] M. Hirata, K. Kokubun, M. Ono, and K. Nakayama, J. Vac. Sci. Technol. A **3**, 1742 (1985).
[10] R. G. Christian, Vacuum **16**, 175 (1966).
[11] H. W. Drawin, Vakuum-Technik, **11**, 45 (1962) (in German).
[12] T. Terasawa, Y. Kawamura, K. Sato, and S. Tanaka, Bull. Jpn. Soc. Prec. Eng. **22**, 49 (1988).
[13] R. A. Buser and N. F. de Rooij, Sensors Actuators **17**, 145 (1989).
[14] K. Kokubun, M. Hirata, M. Ono, H. Murakami, and Y. Toda, J. Vac. Sci. Technol. A **3**, 2184 (1985).
[15] K. Kokubun, M. Hirata, M. Ono, H. Murakami, and Y. Toda, J. Vac. Sci. Technol. A **5**, 2450 (1987).
[16] R. T. Howe and R. S. Muller, IEEE Trans. Electron Devices **ED-33**, 499 (1986).
[17] W. C. Tang, C.-T. H. Nguyen, M. W. Judy, and R. T. Howe, Sensors Actuators, **A21-A23**, 328 (1990).
[18] C. J. van Mullem, F. R. Blom, J. H. J. Fluitman, and M. Elwenspoek, Sensors Actuaturs A **27–29**, 379 (1991).
[19] S. Bouwstra, R. Legtenberg, H. A. C. Tilmans, and M. Elwenspoek, Sensors Actuators A **21-23**, 332 (1990).
[20] C. M. Harris and C. E. Crede, *Shock and Vibration Handbook*, 3rd ed. (McGraw–Hill, New York, 1988).
[21] S. Timoshenko, D. H. Young, and W. Weaver, Jr., *Vibration Problems in Engineering*, 4th ed. (Wiley, New York, 1974), pp. 415–431.
[22] H. Lamb, *Hydrodynamics*, 6th ed. (Cambridge University, Cambridge, 1932).
[23] R. A. Millikan, Phys. Rev. **21**, 1 (1923).
[24] R. A. Millikan, Phys. Rev. **21**, 217 (1923).